SUPPORTING INFORMATION

Fluorinated Aromatic PCBTF and 6:2 diPAP in Bridge and Traffic Paints

Mitchell L. Kim-Fu[1], Ansel R. Moll[2], Esteban E. Hernandez[1], Boris Droz[3], Thierry N.J. Fouquet[4], Jennifer A. Field[5,*]

[1]Department of Chemistry, Oregon State University, Corvallis, OR 97331, USA

[2]School of Chemical, Biological, and Environmental Engineering, Oregon State University, Corvallis, OR 97331, USA

[3]Department of Biological and Ecological Engineering, Oregon State University, Corvallis, OR 97331, USA

[4]Bausch + Lomb Americas, Rochester, NY 14609, USA

[5]Department of Environmental and Molecular Toxicology, Oregon State University, Corvallis, OR 97331, USA

[*]Corresponding Author

Email Address: jennifer.field@oregonstate.edu; Phone: (541) 737-2265; Fax: (541) 737-0497

Number of Pages: 25

Number of Tables: 7

Number of Figures: 10

Table of Contents **Page**

Materials. High performance HPLC grade water (>99%) and methanol for nonvolatile PFAS analysis (>99%) were purchased from Fisher Scientific (Hampton, NH). Methanol for volatile PFAS analysis (≥99.5%) and ammonium acetate for ionic (non-volatile) PFAS analysis (≥97%) were purchased from VWR (Radnor, PA). Deuterated methanol (99.8%) for ^{19}F-NMR was purchased from Cambridge Isotope Laboratories (Tewksbury, MA). Deuterated TFE (d_3-TFE) was purchased from Sigma-Aldrich (St. Louis, MO).

GC-MS Analysis. For volatile PFAS and *p*-chlorotrifluorobenzene (PCBTF) analysis, 10 µL of extract was injected in splitless mode with an inlet temperature of 280 °C. A 4 mm i.d. single taper Topaz inlet liner with 15 mg deactivated quartz wool (Restek, Bellefonte, PA) was used. Helium was used as the carrier gas in a constant flow mode of 1 mL/min. Separations were performed using a deactivated, fused silica tubing capillary column (Agilent, 5 m × 0.53 mm i.d.) connected to an Rxi-624Sil MS capillary column (Restek, 30 m ×0.25 mm i.d., 1.40 µm film thickness). The GC oven temperature program was as follows: 50 °C for 2 min, ramped to 188 °C at a rate of 5 °C/min, then ramped to 300 °C at a rate of 15 °C/min for a total run time of 37.07 min. The Agilent 6890 GC was connected to an Agilent 5973N MS (Santa Clara, CA) that was operated in positive chemical ionization mode and in selected ion monitoring mode with methane as the reagent gas at a flow rate of 1 mL/min. Analyte concentrations for fluorotelomer alcohols (FTOHs), secondary fluorotelomer alcohols (sFTOHs), perfluoroalkyl sulfonamides (FOSAs), and perfluoroctane sulfonamidoethanols (FOSEs) were determined by a calibration curve with a minimum of 6 points with 1/x weighted linear regression or quadratic regression. All standards were prepared in the range of 1–2000 pg/µL. For PCBTF, due to the lack of a matching internal standard and large response, an external calibration curve of 6 points using linear regression was used for quantification. The PCBTF calibration curve was prepared in the range of 1–500 pg/µL. Continuing calibration verification standards (10 and 100 pg/µL) were analyzed after every five paint samples and concentrations were expected to fall within ±30%. Method blanks and solvent blanks were analyzed to monitor potential carryover introduced during the experimental procedure; however, none was observed.[1] Method accuracy and precision for volatile PFAS were determined by spiking three replicates of a blank paint (20 mg in 1500 µL methanol) to give a final concentration vial of 100 pg/µL of target FTOHs, sFTOHs, FOSAs, and FOSEs. For PCBTF, method accuracy and precision was determined by spiking three replicates of a blank paint (20 mg

in 1500 µL methanol) to give a final vial concentration of 50 pg/µL. Whole-method LODs and LOQs were determined using the method of Vial and Jardy.[2] Eight blank (TP-L) paint samples were spiked with target FTOHs, sFTOHs, FOSAs, FOSEs, and PCBTF to give concentrations ranging from 0.17 – 420 pg/µL. Samples were then treated by the same procedure for liquid paint by GC-MS analysis. The LOD was calculated based on weighted linear regression and method LOQ was calculated by multiplying LOD by 3.3.[2]

LC-QTOF Analysis. Chromatographic separations were achieved using an Agilent 1260 HPLC (Santa Clara, CA). Aliquots of 100 µL of sample were injected onto a Zorbax Eclipse XDB-C8 (Agilent, 4.6 × 20 mm, 3.5 µm) guard column fitted with a Zorbax Eclipse Plus C18 analytical column (Agilent, 4.6 × 75 mm, 3.5 µm) as modified after Backe et al (2013).[3] The aqueous mobile phase (A) was 20 mM ammonium acetate (Fisher Scientific, Hampton, NH) in 3% v/v HPLC-grade methanol in HPLC-grade water and the organic mobile phase (B) was HPLC-grade methanol. An AB SCIEX X500R QTOF-MS/MS system (Framingham, MA) was operated in negative mode (ESI-) and positive mode (ESI+) in electrospray ionization. Data were collected under SWATH® data-S5 independent acquisition for both TOF-MS and MS/MS modes. Both PFBA and MPFBA were analyzed in MS/MS mode to reduce background interferences. Over the entirety of the data acquisition period, precursor ion data (TOF-MS) were collected over an m/z range of 100 Daltons (Da; TOF start mass) to 1250 Da (TOF stop). The accumulation time was 200 ms and the ion spray voltage was -4500 V. The source and gas parameters were: 550 °C source temperature, 60 psi ion source gasses, 35 psi curtain gas, and 10 psi collision gas. The declustering potential was -20 V with 0 V spread and the collision energy was -5 V with 0 V spread. Fragments obtain by collision-induced dissociated (CID) data were collected over an m/z range from 50 Da (TOF start mass) to 1200 Da (TOF stop). The accumulation time for each SWATH window was 50 ms. Identification and quantification of target PFAS was described in Schwichtenberg et al. [4] Calibration curves were weighted 1/x or $1/x^2$ and made with a minimum of 5 points over the range. In negative mode the calibration range was 200-50,000 ng/L. The mass labeled internal standards used for quantification of each target ionoic PFAS are listed in **Table S2**. For negative mode analyses, values for a third-party reference standard (Absolute Standards, Hamden, CT) containing carboxylates (C6-14), sulfonates (C4, 6, 8), MeFOSAA, and EtFOSAA were required to fall within ±30% of the expected values. In positive mode, the calibration curves ranged from 200-50,000

ng/L for the five positive mode standards (PFSxSaAm, 6:2 FTSAB, N-Tamp-FHxSA, 5:3 FTB, and 5:1:2 FTB) and the d3-prometon internal standard (**Table S2**). For both negative and positive mode, continuing calibration verification standards consisting of 500 ng/L and 2,000 ng/L were analyzed every five samples and required to fall within ±30% of the expected value. Whole-method LODs and LOQs were determined using the method of Vial and Jardy.[2] Seven blank (TP-L) paint samples were spiked with target ionic PFAS to give final vial concentrations ranging from 8.3-833 ng/L. Samples were then treated by the same procedure for liquid paint by LC-QTOF analysis. The LOD was calculated based on weighted-linear regression and method LOQ was calculated by multiplying LOD by 3.3.[2] The QTOF resolution in negative mode at m/z 520 is 28000 with a maximum retention time deviation and mass error of 0.08 min and 4.9 ppm, respectively. For positive mode, the resolution at m/z 610 is 33000 with a maximum retention time deviation and mass error of 0.04 min and 0.9 ppm, respectively.

Suspect Screening. PatRoon (v2.3.1)[5] non-target analysis (NTA) workflows for environmental analysis was used under R (4.3.2)[6] environment. First, high-resolution mass spectrometry data files were converted into mzXML format using Proteowizard MSconvert (v3.0).[7] Peak picking and alignment were made using XCMS[8] with optimized parameters to perform best-feature finding using the Isotopologue Parameter Optimization (IPO) algorithm.[9] Only features appearing in all triplicates, with at least 1000 area counts and having area counts at least three-time higher compared to the method blanks were considered for further analysis. A couple of tools were taking in account and combined through PatRoon to increase the confidence level on annotated compounds using MS2 data. First, MS2 peak list were annotated for formula using Genform.[10] Then, in silico fragmentation and matched against mass to charge values was performed using MetFrag CL (v2.5.0)[11] using a dedicate database for PFAS.[12] Final annotation using NIST MS2 PFAS library (v1.1) was made.[13] Suspects were screened using the NIST (v1.8)[14] suspect list. Then, negative and positive list were created by selecting the compounds containing a proton donors or acceptor only, respectively using the RDKit tools.[15] Identification confidence follow established criteria.[16]

^{19}F-NMR Analysis. The NMR experiments were conducted using a Bruker 800 MHz Avance IIIHD NMR spectrometer equipped with a 5 mm TCI cryoprobe tuned to ^{19}F. Data were collected with a calibrated 90-degree pulse of 11 µs, a spectral window of 237.2 ppm, 65536 complex points, and a 15 s recycle delay. Experiments were collected in automation using a refrigerated SampleCase and IconNMR software (Bruker, Billerica, MA). Spectra were referenced to $CFCl_3$ by adjusting the d_3-trifluoroethanol (TFE) resonance to 76.76 ppm. To determine the limits of detection (LOD) and quantification (LOQ) seven TFE standards in d_4-methanol ranging in concentration from 410 µg/L to 2400 µg/L were treated by weighted linear regression and method LOQ was calculated by multiplying LOD by 3.3.[2]

Determination of Total Fluorine using NMR. Total area units associated with fluorine were calculated according to **Equation S1**:

$$Area_{Fluorine} = \left(Area_{total} - Area_{TFE\ IS} - \left(Area_{noise} \times 4\right)\right) \qquad \textbf{Eqn S1}$$

Total fluorine concentrations were calculated according to **Equation S2**:

$$\Sigma[F] = Area_{Fluorine} \times \frac{[TFE\ IS] \times n_F}{Area_{\ TFE\ IS}} \times DF \qquad \textbf{Eqn S2}$$

where:

$Area_{Fluorine}$: Total Integrated Area of -CF_2 and -CF_3 Groups (-70 to -200 ppm)

$Area_{total}$: Total Integrated Area of ^{19}F Spectrum (0 to -200 ppm)

$Area_{TFE}$: Total Integrated Area of Internal Standard TFE (-76.73 to -76.82 ppm)

$Area_{Fluoride}$: Total Integrate Area of Fluoride (-121.67 to -121.85 ppm)

$Area_{noise}$: A Portion of the Total Integrated Area due to Instrument Noise (0 to -50 ppm)

$\Sigma[F]$: Total Fluorine Concentration (mM F)

$[TFE\ IS]$: TFE Internal Standard Concentration (mM)

n_F: Number of F atoms in TFE

DF: Dilution Factor

Calculation of Potential Amount 6:2 diPAP per Marking Type. Estimation of 6:2 diPAP contribution per mile of road was done using estimated density of paint (ρ_{paint}=1.2 g mL^{-1}) by the

NIH[17] and liters of paint per kilometer of road dependent on traffic marking type estimated by the Ohio Department of Transportation.[18]

$$[\text{6:2 diPAP}]\frac{\mu\text{g 6:2 diPAP}}{\text{g Paint}} \times \frac{10^6\ \text{g 6:2 diPAP}}{\mu\text{g 6:2 diPAP}} \times \rho_{paint}\frac{\text{g paint}}{\text{mL Paint}} \times \frac{1000\ \text{mL}}{1\ \text{L}} \times \frac{\text{L paint}}{\text{km Road}} \quad \textbf{Eqn S3}$$

EGA-MS and py-GC-MS Analysis. The GC inlet (temperature: 325 °C, split ratio: 1:50) was connected to the splitter using a 1.2 m x 200 µm deactivated capillary attached to a using grade 5.0 helium as carrier gas at 1.5 mL/min in constant flow mode and heated at a constant 250 °C with the GC oven. For py-GC analyses, the pyrolyzer temperature was set at 600 °C which is high enough to decompose all the paints and reference fluorinated polymers but lower than the decomposition temperature of the inorganic fillers releasing CO_2 as observed for all but one paint samples in the EGA-MS analyses. The GC inlet (temperature: 325 °C, split ratio: 1:50) was connected to the splitter using a Restek DB-5 (30 m x 250 µm x 0.25 µm) column using helium as carrier gas at 1.5 mL/min in constant flow mode. The GC oven temperature program was as follows: 40 °C for 3 min followed by a single ramp at 20 °C per min to 320 °C held for 8 min. For all experiments, the splitter was connected to the mass spectrometer using a 2 m x 150 µm x 0 µm restrictor with helium as carrier gas at a constant 1.25 mL/min flow rate. The mass spectrometer was operated in EI mode (source temperature: 250 °C emission: 1.5 µA; energy: 70eV), acquiring signal from m/z 40 to m/z 950 at a rate of 5 scans/sec and a threshold of 10 counts. The system was controlled by MassHunter 10.0 (Agilent) and Maestro 1.5 (Gerstel). The data files .d generated by the instrument were converted to .mzML using msConvert and processed using Bokbunja 2.11. The data processing consisted in A) a blank subtraction using the EGA-MS or py-GC-MS TIC of the conditioned empty quartz tube prior to add the sample as blank to remove the contribution of semi-volatile hydrocarbon contaminants in EGA and of column bleed in py-GC-MS (tolerance: ±2.5 mDa, **Fig. S9**), and B) the automatic extraction of all $–(CF_2)_n–$ series with $n\geq2$ (threshold: 5e3, tolerance ±5 mDa) from the blank-subtracted TICs. The blank subtraction also reduces the total number of points per data file, thus accelerating the extraction step.

Results and Discussion

py-GC-MS. Methyl methacrylate is detected as the main component of all but one paint samples in their pyrograms. Additionally, TP-M and BP-2 then follow in terms of similarity with MMA, methylene heptane (or isomer) and styrene as the main compounds, although the pyrogram of BP-2 also indicates the presence of isocyanate as marker of polyurethane resin, similarly to the most distinct paint sample BP-1. In all cases, however, not a single CF_2 feature was extracted from the pyrograms of the paint samples using Bokbunja while the extraction of $(CF_2)_n$ series from the pyrograms of the reference polymers using the same processing technique returned once again more than 90% of the blank-subtracted TICs. Besides usual organic polymer bases, such as poly(methyl methacrylate) or polyurethane, or inorganic fillers such as calcium carbonate, no noticeable contribution of a fluoropolymer could thus be found in these solid paint residues. The EGA-MS profiles could be separated into two groups. The first group (samples TP-B, TP-C, TP-H, and TP-M) shows a quasi-single release of decomposition products with a maximum of T=390 °C. The second group (BP-1 and BP-2) shows multiple releases of decomposition products over a broad range of temperatures with multiple maxima.

EGA-MS. As observed in the EGA-MS TIC, a large amount of carbon dioxide is released at high temperature from the decomposition of the inorganic filler of BP-1. It leads to an excessively broad peak in the early elution times of the pyrogram, suppressing potential fluorinated species expected to elute within the same time range. The temperature of pyrolysis for paint and reference fluorinated samples has thus been reduced to 600°C, higher than the highest decomposition temperature of all the samples as found from their EGA-MS TICs, but lower than the decomposition temperature of the inorganic fillers (**Figure S10**).

Table S1. List of target volatile PFAS analytes. All standards were purchased from Wellington Laboratories (Guelph, ON, Canada) except for PCBTF which was purchased from ThermoScientific (Waltham, MA, USA).

Analyte	Acronym	Neutral Molecular Formula	Quantifier Ion (*m/z*)	Qualifier Ion (*m/z*)	Extracted Internal Standard
4:2 fluorotelomer alcohol	4:2 FTOH	$C_6H_5OF_9$	265	227	MFBET
5:2 secondary fluorotelomer alcohol	5:2 sFTOH	$C_7H_5OF_{11}$	277	315	MFBET
6:2 fluorotelomer alcohol	6:2 FTOH	$C_8H_5OF_{13}$	365	327	MFHET
7:2 secondary fluorotelomer alcohol	7:2 sFTOH	$C_9H_5OF_{15}$	377	415	MFHET
8:2 fluorotelomer alcohol	8:2 FTOH	$C_{10}H_5OF_{17}$	465	427	M2FOET
10:2 fluorotelomer alcohol	10:2 FTOH	$C_{12}H_5OF_{21}$	565	527	MFDET
12:2 fluorotelomer alcohol	12:2 FTOH	$C_{14}H_5OF_{25}$	665	627	MFDET
N-methyl perfluoroalkane sulfonamide	MeFOSA	$C_9H_4NO_2SF_{17}$	514	-	d_3-N-MeFOSA-M
N-ethyl perfluoro-1-octane sulfonamide	EtFOSA	$C_{10}H_6NO_2SF_{17}$	528	-	d_5-N-EtFOSA-M
N-methyl perfluorooctane sulfonamidoethanol	MeFOSE	$C_{11}H_8NO_3SF_{17}$	540	558	d_7-N-MeFOSE-M
N-ethyl perfluorooctane sulfonamidoethanol	EtFOSE	$C_{12}H_{10}NO_3SF_{17}$	554	572	d_9-N-EtFOSE-M
p-chlorotrifluorobenzene	PCBTF	$C_7H_4ClF_3$	181	-	-

Table S2. List of suspect volatile PFAS analytes.

Analyte	Acronym	Neutral Molecular Formula	Quantifier Ion (*m/z*)	Qualifier Ion (*m/z*)	Extracted Internal Standard
14:2 fluorotelomer alcohol	14:2 FTOH	$C_{16}H_5OF_{29}$	765	727	MFDET
N-methyl perfluoropropane sulfonamidoethanol	MeFPrSE	$C_6H_8NO_3SF_7$	290	308	d_7-N-MeFOSE-M
N-methyl perfluorobutane sulfonamidoethanol	MeFBSE	$C_7H_8NO_3SF_9$	340	358	d_7-N-MeFOSE-M
N-methyl perfluoropentane sulfonamidoethanol	MeFPeSE	$C_8H_8NO_3SF_{11}$	390	408	d_7-N-MeFOSE-M
N-methyl perfluorohexane sulfonamidoethanol	MeFHxSE	$C_9H_8NO_3SF_{13}$	440	458	d_7-N-MeFOSE-M
N-methyl perfluoroheptane sulfonamidoethanol	MeFHpSE	$C_{10}H_8NO_3SF_{15}$	490	508	d_7-N-MeFOSE-M
N-ethyl perfluoroethane sulfonamidoethanol	EtFEtSE	$C_6H_{10}NO_3SF_5$	254	272	d_9-N-EtFOSE-M
N-ethyl perfluoropropane sulfonamidoethanol	EtFPrSE	$C_7H_{10}NO_3SF_7$	304	322	d_9-N-EtFOSE-M
N-ethyl perfluorobutane sulfonamidoethanol	EtFBSE	$C_8H_{10}NO_3SF_9$	354	372	d_9-N-EtFOSE-M
N-ethyl perfluoropentane sulfonamidoethanol	EtFPeSE	$C_9H_{10}NO_3SF_{11}$	404	422	d_9-N-EtFOSE-M
N-ethyl perfluorohexane sulfonamidoethanol	EtFHxSE	$C_{10}H_{10}NO_3SF_{13}$	454	472	d_9-N-EtFOSE-M
N-ethyl perfluoroheptane sulfonamidoethanol	EtFHpSE	$C_{11}H_{10}NO_3SF_{15}$	504	522	d_9-N-EtFOSE-M

Table S3. List of target ionic (nonvolatile) PFAS analytes.

Analyte	Acronym	Neutral Molecular Formula	Internal Standard
Perfluoro-n-butanoic acid	PFBA[2]	$C_4HO_2F_7$	MPFBA
Perfluoro-n-petnanoic acid	PFPeA	$C_5HO_2F_9$	M3PFPeA
Perfluoro-n-hexanoic acid	PFHxA	$C_6HO_2F_{11}$	M2PFHxA
Perfluoro-n-heptanoic acid	PFHpA	$C_7HO_2F_{13}$	M4PFHpA
Perfluoro-n-octanoic acid	PFOA	$C_8HO_2F_{15}$	M4PFOA
Perfluoro-n-nonanoic acid	PFNA	$C_9HO_2F_{17}$	M5PFNA
Perfluoro-n-decanoic acid	PFDA	$C_{10}HO_2F_{19}$	MPFDA
Perfluoro-n-undecanoic acid	PFUdA	$C_{11}HO_2F_{21}$	MPFUdA
Perfluoro-n-dodecanoic acid	PFDoA	$C_{12}HO_2F_{23}$	MPFDoA
Perfluoro-n-tridecanoic acid	PFTrDA	$C_{13}HO_2F_{25}$	MPFDoA
Perfluoro-n-tetradecanoic acid	PFTeDA	$C_{14}HO_2F_{27}$	M2PFTeDA
Perfluoro-n-hexadecanoic acid	PFHxDA	$C_{16}HO_2F_{31}$	M2PFHxDA
Perfluoropropane sulfonate	PFPrS	$C_3HO_3SF_7$	M3PFBS
Perfluorobutane sulfonate	PFBS	$C_4HO_3SF_9$	M3PFBS
Perfluoropentane sulfonate	PFPeS	$C_5HO_3SF_{11}$	M3PFBS
Perfluorohexane sulfonate	PFHxS	$C_6HO_3SF_{13}$	MPFHxS
Perfluoroheptane sulfonate	PFHpS	$C_7HO_3SF_{15}$	MPFHxS
Perfluorooctane sulfonate	PFOS	$C_8HO_3SF_{17}$	MPFOS
Perfluorononane sulfonate	PFNS	$C_9HO_3SF_{19}$	MPFOS
Perfluorodecane sulfonate	PFDS	$C_{10}HO_3SF_{21}$	MPFOS
Perfluorododecane sulfonate	PFDoS	$C_{12}HO_3SF_{25}$	MPFOS
8-chloro-perfluorooctane sulfonate	Cl-PFOS	$C_8HClF_{16}SO_3$	MPFOS
Perfluoroethylcyclohexane sulfonate	PFEtCHxS	$C_8HO_3SF_{15}$	MPFHxS
Perfluorobutane sulfonamide	FBSA	$C_4H_2O_2NSF_9$	M8FOSA
Perfluorohexane sulfonamide	FHxSA	$C_6H_2O_2NSF_{13}$	M8FOSA
Perfluorooctane sulfonamide	FOSA	$C_8H_2O_2NSF_{17}$	M8FOSA
N-methylperfluoro-1-octane sulfonamide	MeFOSA	$C_9H_4O_2NSF_{17}$	d-N-MeFOSA-M
N-ethylperfluoro-1-octane sulfonamide	EtFOSA	$C_{10}H_6O_2NSF_{17}$	d-N-EtFOSA-M
Perfluorooctane sulfonamido acetic acid	FOSAA	$C_{10}H_4O_4NSF_{17}$	d_3-N-MeFOSAA
N-methylperfluorooctane sulfonamido acetic acid	MeFOSAA	$C_{11}H_6O_4NSF_{17}$	d_3-N-MeFOSAA
N-ethylperfluorooctane sulfonamido acetic acid	EtFOSAA	$C_{12}H_8O_4NSF_{17}$	d5-N-EtFOSAA
4:2 fluorotelomer sulfonate	4:2 FTS	$C_6H_5O_3SF_9$	M2-4:2FTS
6:2 fluorotelomer sulfonate	6:2 FTS	$C_8H_5O_3SF_{13}$	M2-6:2FTS
8:2 fluorotelomer sulfonate	8:2 FTS	$C_{10}H_5O_3S_{F17}$	M2-8:2FTS

Analyte	Acronym	Neutral Molecular	Internal

		Formula	Standard
10:2 fluorotelomer sulfonate	10:2 FTS	$C_{12}H_5O_3SF_{21}$	M2-8:2FTS
6:2 fluorotelomer carboxylic acid	6:2 FTCA	$C_8H_3O_2F_{13}$	M6:2FTA
8:2 fluorotelomer carboxylic acid	8:2 FTCA	$C_{10}H_3O_2F_{17}$	M8:2FTA
10:2 fluorotelomer carboxylic acid	10:2 FTCA	$C_{12}H_3O_2F_{21}$	M10:2FTA
3:3 fluorotelomer carboxylic acid	3:3 FTCA	$C_6H_5O_2F_7$	M6:2FTA
5:3 fluorotelomer carboxylic acid	5:3 FTCA	$C_8H_5O_2F_{11}$	M8:2FTA
7:3 fluorotelomer carboxylic acid	7:3 FTCA	$C_{10}H_5O_2F_{15}$	M10:2FTA
2H-Perfluoro-2-octenoic acid (6:2)	6:2 UFTCA	$C_8H_2O_2F_{12}$	M6:2FTUA
2H-Perfluoro-2-decenoic acid (8:2)	8:2 UFTCA	$C_{10}H_2O_2F_{16}$	M8:2FTUA
Dodecafluoro-3H-4,8-dioxanoate	ADONA	$C_7H_2O_4F_{12}$	M5PFNA
9-chlorohexadecafluoro-3-oxanonane-1-sulfonate	9Cl-PF3ONS	$C_8HF_{16}ClSO_4$	MPFOS
11-chloroeicosafluoro-3-oxaundecane-1-sulfonate	11-PF3OUdS	$C_{10}HF_{20}ClSO_4$	MPFOS
hexafluoropropylene oxide-dimer acid	HFPO-DA	$C_6HF_{11}O_3$	MHFPO-DA
bis(1H,1H,2H,2H-perfluorooctyl)phosphate	6:2 diPAP	$C_{16}H_9F_{26}O_4P$	M4 8:2 diPAP
bis(1H,1H,2H,2H-perfluorodecyl)phosphate	8:2 diPAP	$C_{20}H_9F_{34}O_4P$	M4 8:2 diPAP
Bis-[2-(N-ethyleperflurooctane-1-sulfonamido)ethyl] phosphate	diSAmPAP	$C_{24}H_{19}F_{34}N_2O_8PS_2$	M4 8:2 diPAP
N-(3-dimethylaminopropan-1-yl)-perfluoro-1-hexanesulfonamide	PFHxSaAm	$C_{11}H_{13}F_{13}N_2O_2S$	d_3-prometon
1-Propanaminium, N-(carboxymethyl)-N,N-dimethyl-3- [[(3,3,4,4,5,5,6,6,7,7,8,8,8-tridecafluorooctyl)sulfonyl]amino]-	6:2 FtSaB	$C_{15}H_{19}F_{13}N_2O_4S$	d_3-prometon
N-[3-(perfluoro-1-hexanesulfonamido)propan-1-yl]-N,N,N-trimethylammonium	N-TAmP-FHxSA	$C_{12}H_{15}F_{13}N_2O_2S$	d_3-prometon
2-[(4,4,5,5,6,6,7,7,8,8,8-Undecafluorooctyl)dimethylammonio]acetate	5:3 FTB	$C_{12}H_{14}F_{11}NO_2$	d_3-prometon
2-[(3,4,4,5,5,6,6,7,7,8,8,8-Dodecafluorooctyl)dimethylammonio]acetate	5:1:2 FTB	$C_{12}H_{13}F_{12}NO_2$	d_3-prometon

[1][M-H]$^-$ adducts were used for quantification

[2]MRM transitions of 213 → 169 and 217 → 172 were used for quantification of PFBA and MPFBA, respectively, to reduce background.

Table S4. Whole method precision (% RSD), whole method accuracy (% average recovery), LODs, and LOQs for ^{19}F-NMR. In TP-L, a d_3-TFE standard ranging in concentration from 16 µg F/g paint to 950 µg F/g paint was spiked and extracted in d_4-methanol. The LOD (n = 7) was determined weighted linear regression and LOQ was calculated by multiplying LOD with 3.3.[2] For accuracy and precision, 1 mM of PCBTF was spiked into TP-L (n=3) and extracted in d_4-methanol.

Figure of Merit	Value
Limit of Detection (µg F/g paint)	60
Limit of Quantification (µg F/g paint)	200
Accuracy (%)	88
Precision (%RSD)	2.0

Table S5. Whole method precision (% RSD), whole method accuracy (% average recovery), LODs, and LOQs based on liquid paint sample (TP-L) spiked with volatile PFAS. Paint was spiked volatile PFAS for whole method precision and whole method accuracy (n = 3) so that the final vial concentration was 50 µg/L for PCBTF and 100 µg/L for all other volatile PFAS. For LODs/LOQs, volatile PFAS were spiked for final concentrations ranging from 0.17 µg/L to 420 µg/L. The LOD (n = 8) was determined by weighted linear regression and LOQ was calculated by multiplying LOD with 3.3.[2]

Analyte	Whole method precision (% average recovery)	Whole method accuracy (% RSD)	LOD (µg/g)	LOQ (µg/g)
4:2 FTOH	130	4.2	1.9	5.7
5:2 sFTOH	110	8.8	1.3	3.9
6:2 FTOH	71	3.0	0.42	1.3
7:2 sFTOH	99	10.	1.3	3.9
8:2 FTOH	71	1.4	0.12	0.36
10:2 FTOH	130	4.7	0.34	1.0
12:2 FTOH	120	6.0	1.3	3.9
MeFOSA	130	2.8	0.22	0.65
EtFOSA	130	1.6	0.28	0.84
MeFOSE	93	1.4	1.6	4.7
EtFOSE	110	3.3	1.7	5.0

Table S6. Volatile PFAS extracted internal standards percent recovery on matrix spike and samples. The recovery of volatile extracted internal standard (EIS) was determined based on the response of each EIS standard relative to the response of 7:1 FTOH as the non-extracted internal standard (NIS). All EIS standard recoveries fall within the ±30% accuracy range except for MFHET. Variation in recovery and 160% recovery for MFHET may be due to the lack of a matching NIS.

Extracted Internal Standard	Average Percent Recovery	% RSD
MFBET	78	13
MFHET	160	13
M2FOET	130	2.2
MFDET	120	4.9
d_3-N-MeFOSA-M	71	15
d_5-N-EtFOSA-M	73	14
d_7-N-MeFOSE-M	110	16
d_9-N-EtFOSE-M	89	15

Table S7. Whole method precision (% RSD), whole method accuracy (% average recovery), LODs, and LOQs based on liquid paint sample (TP-L) spiked with ionic (non-volatile) PFAS. Painted was spiked with non-volatile PFAS for whole method precision and whole method accuracy (n = 3) so that the final concentration was 833 ng/L. For LODs/LOQs, non-volatile PFAS were spiked for final vial concentrations ranging from 8.3 ng/L to 833 ng/L. The LOD (n = 7) was determined by weighted linear regression and LOQ was calculated by multiplying LOD with 3.3.[2]

Analyte	Whole method precision (% average recovery)	Whole method accuracy (% RSD)	LOD (µg/g)	LOQ (µg/g)
PFBA	130	13	0.037	0.11
PFPeA	110	14	0.013	0.039
PFHxA	100	6.8	0.0031	0.0094
PFHpA	120	6.5	0.0042	0.013
PFOA	110	11	0.0041	0.012
PFNA	100	6.4	0.011	0.033
PFDA	99	11	0.0093	0.028
PFUdA	110	7.0	0.0087	0.026
PFDoA	98	7.8	0.0094	0.028
PFTrDA	76	14	0.0093	0.028
PFTeDA	100	5.9	0.0099	0.030
PFHxDA	110	7.5	0.0058	0.017
PFPrS	110	16	0.0071	0.021
PFBS	270	20	0.86	2.6
PFPeS	96	14	0.0026	0.0077
PFHxS	100	7.3	0.0068	0.021
PFHpS	100	7.7	0.0017	0.0051
PFOS	110	6.8	0.0091	0.027
PFNS	98	6.1	0.0024	0.0072
PFDS	93	4.3	0.0048	0.014
PFDoS	75	8.5	0.00059	0.0018
Cl-PFOS	110	7.7	0.0021	0.0064
PFEtCHxS	98	8.6	0.0078	0.024
FBSA	110	4.4	0.0060	0.018
FHxSA	110	3.1	0.0029	0.0088
FOSA	120	6.3	0.0020	0.0060
MeFOSA	100	9.9	0.0012	0.0035
EtFOSA	110	13.6	0.0050	0.015
FOSAA	73	12	0.0015	0.0046
MeFOSAA	110	6.7	0.00041	0.0012
EtFOSAA	110	7.7	0.011	0.034
4:2 FTS	77	28	0.013	0.040
6:2 FTS	110	7.1	0.0039	0.012
8:2 FTS	130	10.	0.012	0.035

Analyte				
10:2 FTS	120	3.3	0.0079	0.024
3:3 FTCA	110	11	0.029	0.086
5:3 FTCA	99	14	0.00016	0.00048
7:3 FTCA	120	22	0.0205	0.048
6:2 FTCA	96	18	0.021	0.061
8:2 FTCA	120	12	0.013	0.039
10:2 FTCA	120	4.2	0.014	0.042
6:2 UFTCA	120	4.0	0.0097	0.029
8:2 UFTCA	120	8.7	0.014	0.043
ADONA	110	5.8	0.0048	0.014
9Cl-PF3ONS	100	7.5	0.0046	0.014
11-PF3OUdS	84	14	0.014	0.041
HFPO-DA	87	9.8	0.019	0.057
6:2 diPAP	114	10.	0.016	0.049
8:2 diPAP	120	7.2	0.0052	0.016
diSAmPAP	56	1.0	0.0029	0.0086
PFHxSaAm	120	4.3	0.0053	0.016
6:2 FtSaB	130	9.6	0.0131	0.039
N-TAmP-FHxSA	120	7.0	0.0020	0.0061
5:3 FTB	110	10.	0.010	0.031
5:1:2 FTB	120	3.7	0.0039	0.012

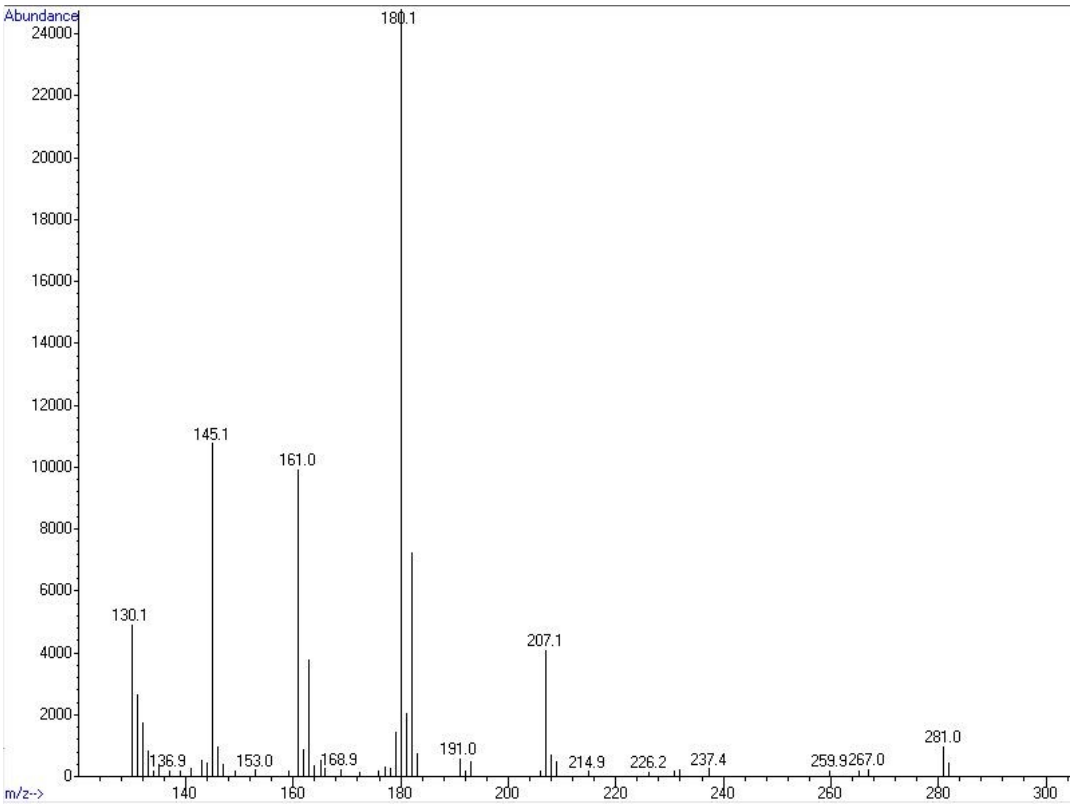

Figure S1. Electron ionization mass spectrum of PCBTF standard acquired in full scan acquisition mode

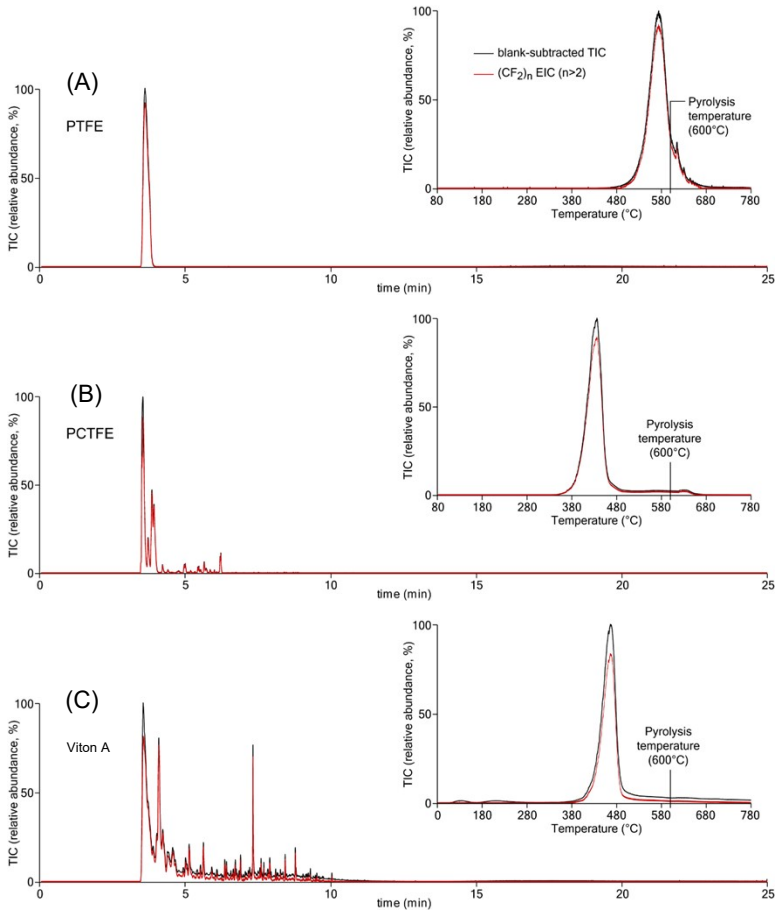

Figure S2. Reference fluoropolymer pyrograms for (a) polytetrafluoroethylene (ThermoFisher, Waltham, MA), (b) poly(chlorotrifluoroethylene) (St. Louis, MO), and (c) Viton A (Chemours, Wilmington, DE).

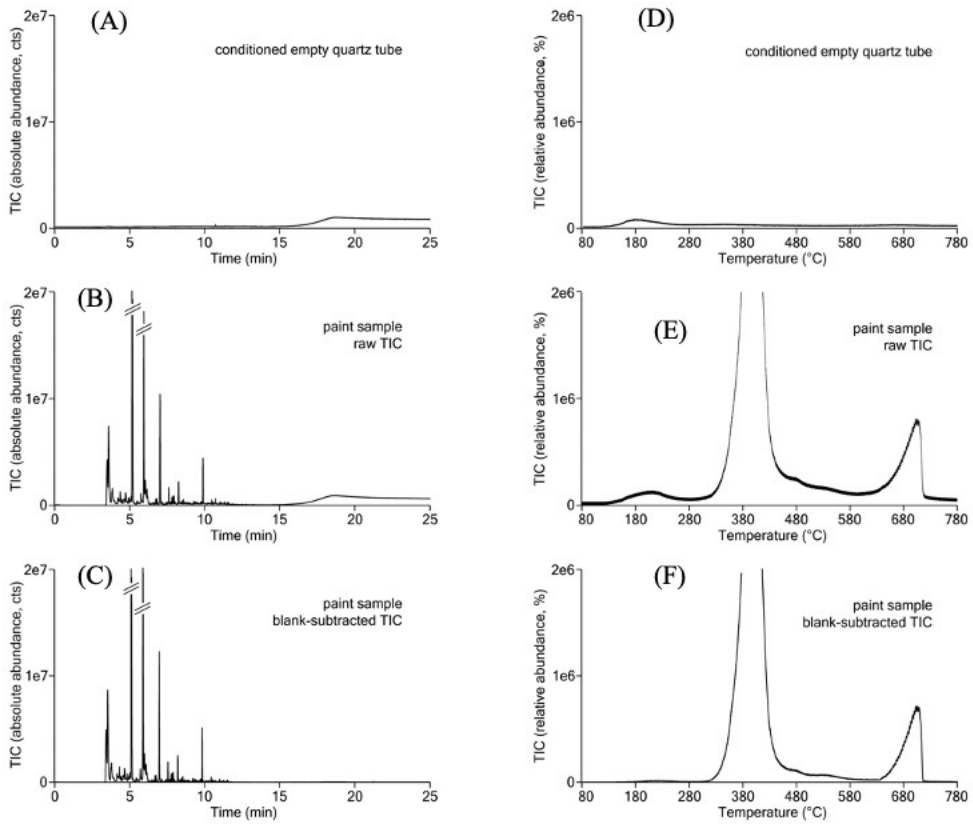

Figure S3. Example of blank subtraction for py-GC-MS TICs (left, (A)-(C)) and EGA-MS (right, (D)-(F)) to reduce the contribution of the column bleed and semi-volatile hydrocarbon contaminants, respectively, while reducing the total number of points to speed up the subsequent extraction of $(CF_2)_n$ series.

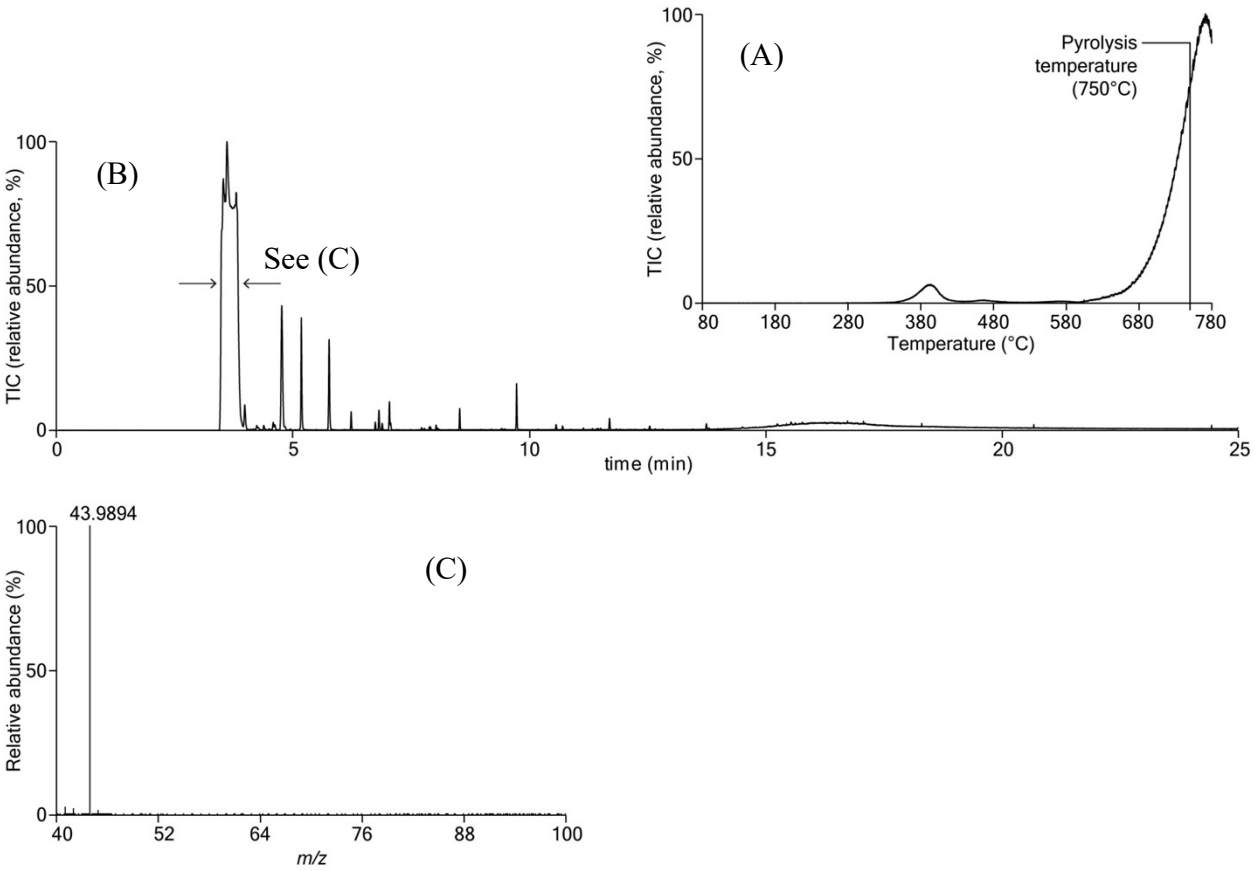

Figure S4. (A) EGA-MS of the paint sample BP-1 and (B) pyrogram from the pyrolysis of BP-1 at 750°C. (C) Average mass spectrum from the first 1.5 min of the pyrogram.

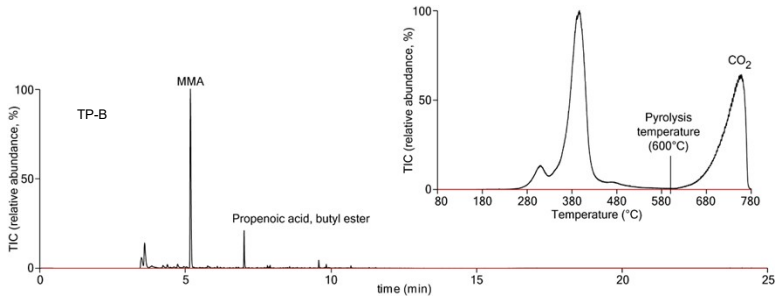

Figure S5. Pyrogram of solid residual from road paint TP-B

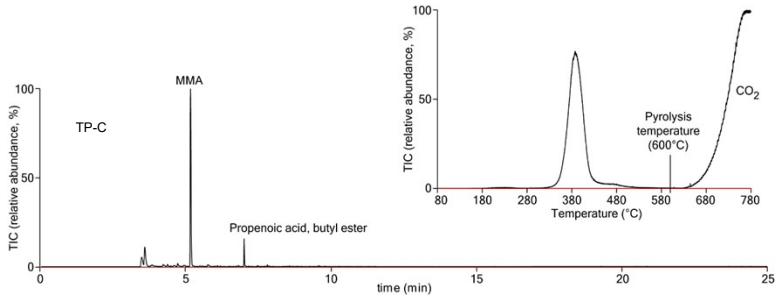

Figure S6. Pyrogram of solid residual from traffic paint TP-C

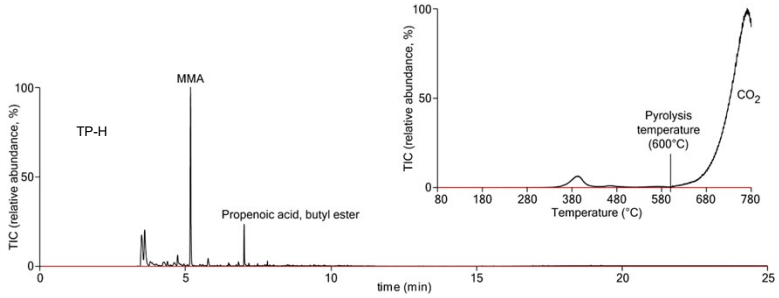

Figure S7. Pyrogram of solid residual from traffic paint TP-H

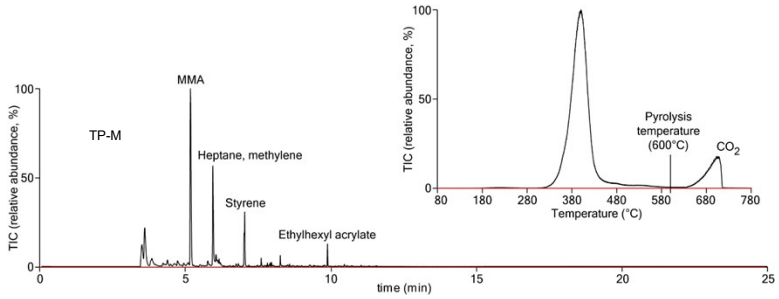

Figure S8. Pyrogram of solid residual from traffic paint TP-M

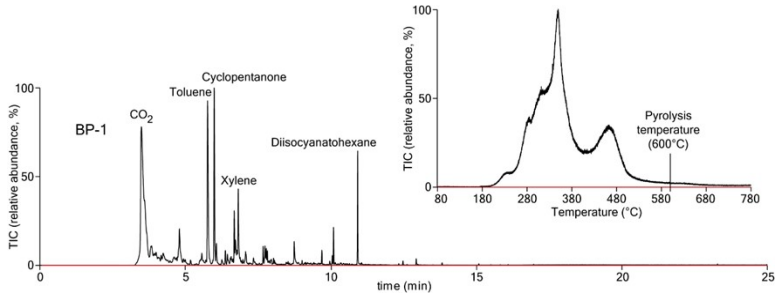

Figure S9. Pyrogram of solid residual from bridge paint BP-1

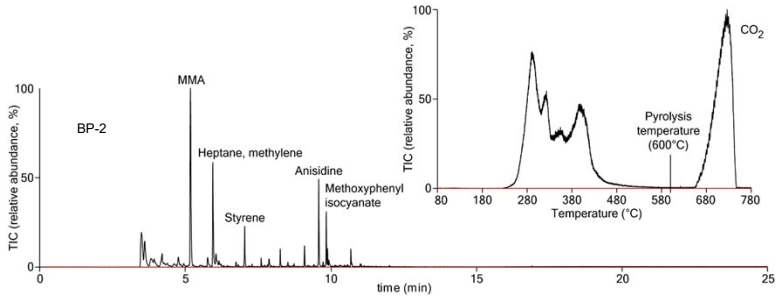

Figure S10. Pyrogram of solid residual from traffic paint BP-2

References

(1) L. Cahuas, I. A. Titaley, J. A. Field, Mass-labeled fluorotelomer alcohol fragmentation gives "false positive" for nonlabeled fluorotelomer alcohols with implications for consumer product analysis, *J. Am. Soc. Mass Spectrom.* 2022, **33**, 399–403.

(2) J. Vial, A. Jardy, Experimental comparison of the different approaches to estimate LOD and LOQ of an HPLC method, *Anal. Chem.* 1999, **71**, 2672–2677.

(3) W. J. Backe, C. T. Day, J. A. Field, Zwitterionic, cationic, and anionic fluorinated chemicals in aqueous film forming foam formulations and groundwater from U.S. military bases by nonaqueous large-volume injection HPLC-MS/MS, *Environ. Sci. Technol.* 2013, **47**, 5226–5234.

(4) T. Schwichtenberg, D. Bogdan, C. C. Carignan, P. Reardon, J. Rewerts, T. Wanzek, J. A. Field, PFAS and dissolved organic carbon enrichment in surface water foams on a Northern U.S. freshwater lake, *Environ. Sci. Technol.* 2020, **54**, 14455–14464.

(5) R. Helmus, B. van de Velde, A. M. Brunner, T. L. ter Laak, A. P. van Wezel, E. L. Schymanski, patRoon 2.0: Improved non-target analysis workflows including automated transformation product screening, *Journal of Open Source Software.* 2022, **7**, 4029.

(6) R: A language and environment for statistical computing, http://www.R-project.org, (accessed 05 May 2024).

(7) D. Kessner, M. Chambers, R. Burke, D. Agus, P. Mallick, ProteoWizard: open source software for rapid proteomics tools development, *Bioinformatics* 2008, **24**, 2534–2536.

(8) C. A. Smith, E. J. Want, G. O'Maille, R. Abagyan, G. Siuzdak, XCMS: processing mass spectrometry data for metabolite profiling using nonlinear peak alignment, matching, and identification, *Anal. Chem.* 2006, **78**, 779–787.

(9) G. Libiseller, M. Dvorzak, U.Kleb, E. Gander, T. Eisenberg, F. Madeo, S. Neumann,G. Trausinger, F. Sinner,T. Pieber, C. Magnes, PO: a tool for automated optimization of XCMS parameters, *BMC Bioinformatics.* 2015, **16**, 118.

(10) M. Meringer, S. Reinker, J. Zhang, A. Muller, MS/MS data improves automated determination of molecular formulas by mass spectrometry. *MATCH Communications in Mathematical and in Computer Chemistry.* 2011, **65**, 259–290.

(11) C. Ruttkies, S. Neumann, S. Posch, Improving MetFrag with statistical learning of fragment annotations, *BMC Bioinformatics.* 2019, **20**, 376.

(12) PubChem OECD PFAS Larger PFAS Parts file for MetFrag (ver. hid120_HNID5525061_20230319) https://doi.org/10.5281/zenodo.7750267, (accessed May 2024).

(13) Database Infrastructure for Mass Spectrometry - Per- and Polyfluoroalkyl Substances - v1.1.0 https://doi.org/10.18434/mds2-2905, (accessed 05 May 2024).

(14) Suspect List of Possible Per- and Polyfluoroalkyl Substances (PFAS*).* https://data.nist.gov/od/id/mds2-2387, (accessed 05 May 2024).

(15) rdkit/rdkit: Release_2023.09.5.*,* https://zenodo.org/records/10633624, (accessed 05 May 2024).

(16) J. A. Charbonnet, C. A. McDonough, F. Xiao, T. Schwichtenberg, D. Cao, S. Kaserzon, K. V. Thomas, P. Dewapriya, B. J. Place, E. L. Schymanski, J. A. Field, D. E. Helbling, C. P. Higgins, Communicating confidence of per- and polyfluoroalkyl substance identification via high-resolution mass spectrometry, *Environ. Sci. Technol. Lett.* 2022, **9**, 473–481.

(17) H. J. Bremmer, J. G. M. van Engelen. Brush and Roller Painting. In *Paint Products Fact Sheet: To assess the risks for the consumer: Updated version for ConsExpo 4*; National Institute for Public Health and the Environment, 2006.

(18) ITEM 642 TRAFFIC PAINT. https://www.dot.state.oh.us/Divisions/ConstructionMgt/OnlineDocs/Specifications/2008CMS/600/642.htm, (accessed 20 December 2023).